A Reduced-Order Two-Degree-of-Freedom Composite Nonlinear Feedback Control for a Rotary DC Servo Motor*

Veli-Pekka Pyrhonen, *Student Member, IEEE*, Hannu J. Koivisto, and Matti K. Vilkko

Abstract— **We study in this paper nonlinear control of a rotary DC servo motor application. To be more specific, we design a reduced-order two-degree-of-freedom (2DOF) composite nonlinear feedback (CNF) controller for a Quanser QUBE-Servo 2 unit with a disc attachment. We compare our results with a carefully tuned proportional-derivative (PD) controller with set point weighting. Our simulation and experimental results show that the closed-loop system using 2DOF CNF controller yields much better set point tracking performance compared with the conventional PD-controller in terms of settling time.**

I. INTRODUCTION

Transient performance is one of the most important characteristics for systems that require fast and precise command following. As regards to tracking step signals, transient performance is commonly measured by rise time, settling time and overshoot. It is well-known that shortening the rise time is usually accompanied by large overshoot, which eventually translates to increased settling time. Therefore, tradeoffs between swiftness and accuracy must be made in any typical controller design task. Furthermore, almost all real systems have limited control authority e.g., control inputs are restricted by actuator saturation constraints, which limit the achievable performance.

Composite nonlinear feedback (CNF) has been proposed to overcome common design tradeoffs in linear control. In general, CNF controllers consist of linear and nonlinear feedback laws such that both laws contribute differently during the transient stage. The design of CNF controllers can be carried out by the following two design principles. First, a lightly-damped linear feedback part is designed for a swift response with large overshoot. Then, the linear feedback law is supplemented by a parallel-connected nonlinear feedback law, which delivers additional damping when the tracking error becomes small. That is, the nonlinear part focuses on the final stage of the transient response by increasing control effort when the output reaches the target reference. Such feature is the key property of CNF control, which effectively shortens the settling time of closed-loop control systems. In fact, additional design freedom can be obtained by fabricating a suitable set point filter, which focuses on the initial stage of the transient response. Such a filter helps to adjust the initial part of the control input as required by the designer.

The CNF methodology was originally proposed by Lin et al. in [1]. Since then, theoretical research has been active in scientific community. For example, Chen et al. laid the foundation for measurement feedback in [2]. Multivariable case was studied by He et al. in [3]. Cheng et al. have generalized CNF control for tracking general references in [4]. Lan et al. have introduced a scaled nonlinear function that achieves robust performance as regards to variation of step magnitude in [5]. Furthermore, Pyrhonen provided conditions for extending CNF control with arbitrary order set point filters, which allowed general dynamic compensators to be used in two-degree-of-freedom (2DOF) setting in [6]. Active theoretical research has resulted in many successful applications of CNF control in different areas of technology. For example, CNF control has been applied to hard disk drives [7–10], gantry crane systems [11], helicopter flight systems [12–14], servo position systems [15–16], robot manipulators [17], and chemical reactors [18].

In this paper, we design a 2DOF CNF controller with a set point filter for a rotary DC servo motor; namely, for a Quanser QUBE-Servo 2 unit. The QUBE-Servo 2 unit is a small-scale testbed intended for education and research, which has two different attachments available for feedback control. We focus in this paper onto angular position control of the rotary disc attachment using an amplitude-constrained actuator. We compare the performance of our 2DOF CNF controller with a well-tuned Proportional-Derivative (PD) controller with set point weighting. We show that the tracking performance of our control system using 2DOF CNF controller is considerably better as opposed to PD-controller in both simulation and experimental setups.

We have organized the material in this paper as follows. In Section 2, we present the design procedure of the 2DOF CNF controller. In Section 3, we apply our method to the angular position control of Quanser QUBE-Servo 2 unit with the disc attachment. Finally, in Section 4, we draw some concluding remarks.

II. TWO-DEGREE-OF-FREEDOM COMPOSITE NONLINEAR FEEDBACK CONTROL

We consider in this paper the following class of SISO (Single-Input-Single-Output) systems with input nonlinearity

$$\begin{cases} \dot{x} = Ax + B\mathrm{sat}(u) \\ y = C_y x \qquad\qquad , \; x(0) = x_0, \\ m = C_m x \end{cases} \qquad (1)$$

V.-P. Pyrhonen, H. J. Koivisto and M. Vilkko are with the Laboratory of Automation and Hydraulics, Tampere University of Technology, PL 692, 33101 Tampere, Finland. (Tel. +358 40 198 1172; e-mail: veli-pekka.pyrhonen@tut.fi; hannu.koivisto@tut.fi; matti.vilkko@tut.fi).

where $x \in \mathbb{R}^n$, $u \in \mathbb{R}$, $y \in \mathbb{R}$ and $m \in \mathbb{R}^p$, $p \leq n$, are the state, control input, controlled output and measured output, whereas x_0 is an initial condition. The actuator saturation constraint is represented by

$$\text{sat}(u) = \min\{u_{\max}, |u|\}\,\text{sgn}(u) , \qquad (2)$$

where $u_{\max}$ is the saturation limit of the input and sgn denotes the sign function. In order to design a CNF controller, the following assumptions must be made

A1: the pair (A, B) is stabilizable;

A2: the pair (A, C_m) is detectable;

A3: the triple (A, B, C_y) is invertible and has no invariant zeros at the origin;

A4: the controlled output y is a subset of m i.e. y is also measured.

In what follows, we present the design procedure of the 2DOF CNF controller with a dynamic set point filter. The procedure can be partitioned in three separate parts, which are: A) the design of a linear state feedback part, B) the design of a linear dynamic feedforward part, and C) the design of a nonlinear state feedback part.

A. Design of Linear State Feedback Part

First, assume that $C_m = I$. Then design a linear feedback law

$$u_L = u_x + u_r = -Kx + R_s r , \qquad (3)$$

where r is the target step reference and K is the full state feedback gain. The gain K should be chosen such that a) all eigenvalues of the matrix $(A - BK)$ have strictly negative real parts, and b) the closed-loop system $C_y(sI - A + BK)^{-1}B$ has a small damping ratio. Then the scalar-valued feedforward gain

$$R_s = -[C_y(A - BK)^{-1}B]^{-1} \qquad (4)$$

assigns unity DC-gain for the model-based closed-loop system from the reference r to the controlled output y. We note that the inner inverse in (4) exists under the given assumptions.

B. Design of Linear Dynamic Feedforward Part

Consider the block diagram in Fig. 1, where an additional proper set point filter $G_f(s)$ is now connected to the reference input path of the closed-loop control system. For a step input $r = a_r r_1$ with a_r being the step amplitude and r_1 the unit step, the feedforward response u_{FF} through the filter and feedforward gain can generally be expressed as
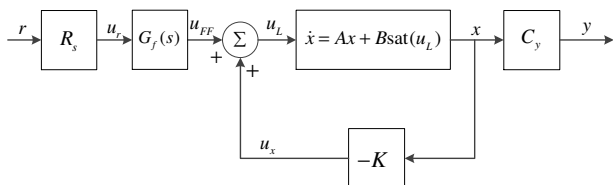

Figure 1. Closed-loop control system with full-state 2DOF controller.

$$u_{FF}(t) = R_s a_r \cdot u_{f,1}(t) , \qquad (5)$$

where $u_{f,1}$ corresponds to the unit step response. The feedforward unit step response through the set point filter is subject to following conditions:

- $u_{f,1} \to 1$ in time i.e. the DC-gain of the filter must be 1.

- $u_{f,1}$ is differentiable from $t > t_s$ onwards, where t_s is the step starting instant.

- $\dot{u}_{f,1}$ is uniformly continuous.

- $\dot{u}_{f,1} \to 0$, $t \to \infty$.

Please refer to [6] for more details. The designer chooses the pole-zero-pattern of the filter such that the decay speed of $u_{f,1}$ is suitable for the closed-loop control system, and, that the magnitude of u_L does not cause actuator saturation. Typically, set point filters are used e.g., to improve the initial stage of the transient response.

C. Design of Nonlinear State Feedback Part

First, specify a desired state x_d using

$$x_d \triangleq R_d a_r \cdot u_{f,1} = -(A - BK)^{-1}BR_s a_r \cdot u_{f,1} . \qquad (6)$$

Then form a 2DOF CNF control law

$$u = u_L + u_N = u_x + u_{FF} + u_N , \qquad (7)$$

where the parallel-connected nonlinear feedback law u_N is given by

$$u_N = \rho(r, y)K_n[x - x_d] = \rho(r, y)B^T P[x - x_d] , \qquad (8)$$

where $P = P^T > 0$, and where $\rho(r, y)$ is any nonpositive function locally Lipschitz in y. The function $\rho(r, y)$ is used to smoothly change the closed-loop damping ratio, when the controlled output y of the system approaches the target step reference r. The matrix P can be obtained by solving the Lyapunov equation

$$(A - BK)^T P + P(A - BK) + Q = 0 \qquad (9)$$

for a given $Q = Q^T > 0$. The solution always exists since $(A - BK)$ is stable.

Next, choose a suitable function $\rho(r, y)$ that is used for increasing the damping ratio of the closed-loop system, when the control error $e \to 0$. In this paper, we select the nonlinear function

$$\rho(e) = -\beta \exp(-\alpha\alpha_0 |e|), \quad |e| = |r - y| , \qquad (10)$$

where

$$\alpha_0 = \begin{cases} 1 / |r - y(0)|, & y(0) \neq r \\ 1, & y(0) = r \end{cases} , \qquad (11)$$

which was originally proposed in [1], and revised in [5]. The function (10) is implementable, because y is part of m.

The revised function (10) is able to adapt for varying step sizes, when CNF controller is commanded to follow non-unit step references. The tuning parameters $\alpha > 0$ and $\beta > 0$ are

chosen such that the closed-loop control system satisfies the desired transient performance requirements i.e., short settling time and small overshoot. Several ways to tune the nonlinear function exists in literature; see, for example: [5; 10]. The design of the 2DOF CNF controller is completed, once the tuning parameters α and β are fixed.

Some important properties of the closed-loop control system comprising the system (1) and the 2DOF CNF controller must be addressed. For such purpose, we restate the following theorem from [6].

Theorem 1. Consider the system (1), the linear control law $u_x + u_{FF}$, and the composite nonlinear feedback law (7). For any $\delta \in (0, 1)$, let $c_\delta > 0$ be the largest positive scalar satisfying

$$\left|Kx\right| \leq u_{\max}(1 - \delta), \ \forall x \in \{x : x^T P x \leq c_\delta\} \triangleq S . \quad (12)$$

Then, the linear control law $u_x + u_{FF}$ tracks the step command $r = a_r r_1$ asymptotically in time without saturating the actuator provided that $x(0)$, $x_d(0)$, a_r and $u_{f,1}$ satisfy:

$$\tilde{x}(0) \triangleq \left(x(0) - x_d(0)\right) \in S \text{ and } \left|a_r\right|\left\|H\right| \cdot \left|u_{f,1}\right| \leq \delta u_{\max}, \ \forall t , \ (13)$$

where

$$H \triangleq -[1 + K(A - BK)^{-1}B]R_s . \quad (14)$$

Furthermore, for any ρ as defined above, the composite nonlinear feedback law in (7) is able to asymptotically track the step command $r = a_r r_1$ provided that (13) is satisfied.

Remark 1. We can show that if the initial condition $x_0 = 0$, then any step amplitude can asymptotically be tracked by the control law $u_x + u_{FF}$ provided that

$$\left|a_r\right| \leq \frac{1}{u_{f,1}(t)}\sqrt{\frac{c_\delta}{R_d^T P R_d}} \text{ and } \left|a_r\right|\left\|H\right| \cdot \left|u_{f,1}\right| \leq \delta u_{\max}, \ \forall t . \quad (15)$$

The result (15) also indicates that we can either increase or decrease the traceable magnitudes of the target step references by utilizing an appropriate set point filter. In either case, the dynamics of $G_f(s)$ should always be faster than the dominating dynamics of the unfiltered closed-loop control system.

Remark 2. A 2DOF CNF controller can be designed under measurement feedback i.e. when $p < n$, if the assumptions A1–A4 are satisfied. Specifically, if the system (1) can be partitioned as

$$\begin{bmatrix} \dot{x}_1 \\ \dot{x}_2 \end{bmatrix} = \begin{bmatrix} A_{11} & A_{12} \\ A_{21} & A_{22} \end{bmatrix}\begin{bmatrix} x_1 \\ x_2 \end{bmatrix} + \begin{bmatrix} B_{11} \\ B_{21} \end{bmatrix}\text{sat}(u) , \quad (16)$$
$$y = C_y x, \ m = C_m x$$

then, a reduced-order 2DOF measurement feedback CNF control law is given by

$$\dot{x}_v = (A_{22} - L_R A_{12})x_v + (B_{21} - L_R B_{11})\text{sat}(u)$$
$$\quad + (A_{21} - L_R A_{11} + (A_{22} - L_R A_{12})L_R)y$$

$$u = K\begin{bmatrix} y \\ x_v + L_R y \end{bmatrix} + G_f(s)R_s r$$

$$+ \rho(e)B^T P\left[\begin{pmatrix} y \\ x_v + L_R y \end{pmatrix} - x_d\right], \quad (17)$$

where the gain L_R is designed such that $(A_{22} - L_R A_{12})$ is stable. We note that CNF control under measurement feedback is discussed in detail in [2], when $G_f(s) \equiv 1$.

III. DESIGN EXAMPLE

In this section, we explain the components and hardware of Quanser QUBE-Servo 2 unit with a rotating disc. We also present the mathematical model of the system along with the control requirements and design constraints. Then, we design a reduced-order 2DOF CNF controller by following the three design steps from the previous section. We compare our controller's tracking performance with Quanser's Workbook PD-controller, which can be found in [19]. Furthermore, we experimentally fine-tune the PD-controller for the fastest possible strictly monotone response. We show that the 2DOF CNF results in much better tracking performance compared with the carefully tuned PD-controller.

A. Quanser QUBE-Servo 2 Unit with Disc Attachment

The QUBE-Servo 2 unit is a small-scale rotary DC motor application, which can serve as a good testbed for control algorithms intended for fast set point tracking. The rotating disc is driven by an Allied Motion CL40 (model 16705) direct-drive 18V brushed DC motor. The DC motor is powered by a Pulse-Width Modulation (PWM) amplifier with integrated current sense. The PWM amplifier receives control commands from Data Acquisition (DAQ) device, which is connected to a PC via USB connection. All controllers in this paper are configured in Matlab/Simulink environment using Quanser Real-Time Control (QUARC) software, which provide necessary blocks to communicate with the servo unit. The QUBE-Servo 2 unit with the disc attachment is depicted in Fig. 2.

The angular position of the rotating disc is measured by a US Digital (model E8P-512-118) relative single-ended rotary optical shaft encoder, which generate 2048 counts per revolution. Such characteristics translate to 0.176 degrees per count accuracy. The motor encoder is connected to the DAQ device, which transmits the output data back to Matlab/Simulink environment via USB connection. The main parameters of the QUBE-Servo 2 device are listed in Table 1.

Figure 2. Quanser QUBE-Servo 2 unit with disc attachment.

TABLE I. QUBE-SERVO 2 DEVICE PARAMETERS

	Symbol	Description	Value
DC-Motor	R_m	Terminal resistance	8.4 Ω
	k_t	Torque constant	0.042 Nm/A
	k_m	Back-emf constant	0.042 V/(rad/s)
	J_m	Rotor inertia	$4.0 \cdot 10^{-6}$ kgm^2
	m_h	Hub mass	0.0106 kg
	r_h	Hub radius	0.0111 m
	J_h	Hub inertia	$0.6 \cdot 10^{-6}$ kgm^2
Disc	m_d	Disc mass	0.053 kg
	r_d	Disc radius	0.0248 m

The dominating dynamics of the QUBE-Servo 2 unit can be derived using first principles modeling, see [19]. The equations of motion are obtained using Kirchoff's law

$$v_m(t) - R_m i_m(t) - k_m \omega_m(t) = 0 , \qquad (18)$$

where v_m is the motor voltage, R_m is the terminal resistance, i_m is the motor current, k_m is the motor back-emf constant, and ω_m is the angular speed of the motor. The motor shaft equation can be expressed as

$$J_{eq} \dot{\omega}_m(t) = \tau_m(t) , \qquad (19)$$

where J_{eq} is the total moment of inertia acting on the motor shaft, and where τ_m is the applied torque from the DC motor. The torque τ_m is given by

$$\tau_m = k_t i_m(t) . \qquad (20)$$

The total moment of inertia is

$$J_{eq} = J_m + J_h + J_d , \qquad (21)$$

where J_m is the rotor inertia, J_k is the hub inertia, and J_d is the disc inertia given by

$$J_d = \frac{1}{2} m_d r_d^2 . \qquad (22)$$

Based on the equations (18)–(22), we can write the following set of first-order ordinary differential equations

$$\begin{bmatrix} \dot{\theta} \\ \dot{\omega} \end{bmatrix} = \begin{bmatrix} 0 & 1 \\ 0 & -k_m k_t / (J_{eq} R_m) \end{bmatrix} \begin{bmatrix} \theta \\ \omega \end{bmatrix} + \begin{bmatrix} 0 \\ k_t / (J_{eq} R_m) \end{bmatrix} \text{sat}(v_m) . \qquad (23)$$

The motor voltage v_m is the control input u, which is limited by $u_{\max} = 15$V.

Unfortunately, we can only measure the relative angular position of the disc attachment θ, which is also the controlled output. Therefore, the output equations are

$$m = y = \begin{bmatrix} 1 & 0 \end{bmatrix} \begin{bmatrix} \theta \\ \omega \end{bmatrix} = \theta, \ m(0) = \theta(0) = 0 . \qquad (24)$$

Nonetheless, it is easy to see that all assumptions A1–A4 are satisfied. Therefore, we can design a reduced-order 2DOF CNF controller for the QUBE-Servo 2 unit. In what follows,

we present the control requirements, design constraints and controller design.

B. Requirements, Constraints and Controller Design

Here, feedback controllers must be designed according to the following requirements and design constraints:

- The set point response should be monotone for a large amplitude step reference;
- The settling time T_s as measured by the 2% criterion should be as short as possible;
- The control input voltage v_m is limited by ±15V;
- The phase margin PM should be ≥ 35 degrees;
- The gain margin GM should be ≥ 2;
- The stability margin s_m should be ≥ 0.5.

We begin by designing the linear feedback part of the 2DOF CNF controller. First, we place the dominating pair of the closed-loop poles at

$$s = -\zeta \omega_n \pm j \omega_n \sqrt{\zeta^2 + 1} = -15 \pm j35 , \qquad (25)$$

which corresponds to the damping ratio $\zeta \approx 0.3939$ and natural frequency $\omega_n \approx 38.08$ rad/s. The chosen pair of poles results in state feedback and reference tracking gains:

$$K = [6.0606 \quad 0.0834] \qquad (26)$$

$$R_s = -[C_y(A - BK)^{-1}B]^{-1} = 6.0606 . \qquad (27)$$

Next, we select an appropriate set point filter that would improve the initial stage of the transient response. It is reasonable to choose the filter dynamics with respect to e.g., the rise time of the unfiltered step response. We find that the rise time T_r of the closed-loop system is approximately 40 milliseconds. We therefore use T_r as a design parameter, and we require that the transient response through the filter converges to the desired value of the given step reference within T_r. The requirement motivates us to select the following set point filter

$$G_f(s) = \frac{0.011s + 1}{0.0091s + 1} , \qquad (28)$$

which completes the design of the linear feedforward part.

In what follows, we design the nonlinear feedback part of the 2DOF CNF controller. For such purpose, we solve the Lyapunov equation (9) for $Q = \text{diag}(15, 1)$, which results in

$$P = \begin{bmatrix} 24.5718 & 0.0052 \\ 0.0052 & 0.0168 \end{bmatrix}, \ P = P^T > 0 . \qquad (29)$$

The gain of the nonlinear part is then given by

$$K_n = B^T P = [1.2375 \quad 4.0288] . \qquad (30)$$

Then we seek suitable tuning parameter values for the nonlinear function (10). It is clear from (10) that the function $\rho \to -\beta$ when $e \to 0$. Therefore, we select the parameter β such that the damping ratio of the closed-loop system is large when the control error becomes small. We select $\beta = 0.16$, which yields the desired result. Then, we need to select the parameter α for appropriate convergence speed when $e \to 0$. Following a few simulation tryouts, we find that $\alpha = 8$ gives

satisfactory performance. Finally, we select the reduced-order observer gain $L_R = 150$. Our reduced-order 2DOF CNF control law is then given by

$$\dot{x}_v = -160.0485x_v + 239.2509\text{sat}(v_m) - 24007\theta, \; x_v(0) = 0$$

$$v_m = -[6.0606 \quad 0.0834]\left[\begin{pmatrix} \theta \\ x_v + 150\theta \end{pmatrix} - x_d\right] + G_f(s)R_s r$$

$$+ \rho(e)B^T P\left[\begin{pmatrix} \theta \\ x_v + 150\theta \end{pmatrix} - x_d\right], \; x_d(0) = [1 \quad 0]^T a_r u_{f,1}(0) \quad (31)$$

with

$$\rho(e) = -0.16\exp(-8\alpha_0|e|), \; e = r - \theta, \; \theta = m = y. \quad (32)$$

We compare the performance of our 2DOF CNF controller with the Quanser's Workbook PD-controller in [19]. The PD-controller in [19] is implemented using position-velocity algorithm, in which the derivative path acts on the negative velocity instead of the velocity of the error. Such construction is equivalent to 2DOF set point weighting, where the error signal $e_c(t) = cr(t) - m(t)$ with $c = 0$ is fed into the derivation channel of the PD-controller. This type of controller is also known as the preceded-derivative PD-controller, see e.g., [20] for more details. The structure of an ideal proportional-velocity controller is

$$u(t) = K_p(r(t) - m(t)) - K_d\dot{m}(t), \quad (33)$$

where K_p is the proportional gain and K_d is the velocity gain. Furthermore, a first-order low-pass filter is used in-line with the derivative action to suppress measurement noise, and to ensure feasible implementation of the derivative action. Therefore, the derivation is implemented through the transfer function

$$G(s) = \frac{s\omega_f}{s + \omega_f}, \quad (34)$$

where ω_f is the cut-off frequency of the filter. In general, the cut-off frequency is chosen such that appropriate filtering is maintained without distracting the signal components of the controlled output. The parameter values for the Quanser's PD-controller are $K_p = 6.10$, $K_d = 0.25$ and $\omega_f = 100$. In what follows, we present our simulation results for the 2DOF CNF controller and for the preceded-derivative PD-controller.

C. Simulation Results

Here, time domain simulations are performed using a step reference with magnitude $a_r = 2$ rad, which is roughly 115 degrees. The step is large enough to utilize full-scale control voltage for the DC motor. We have collected the closed-loop tracking performances in Fig. 3 along with the control components u_x, u_{FF} and u_N. We have recalibrated the gain $R_s = [C_y(A-BK-\beta BB^T P)^{-1}B]^{-1}$ to cancel a small steady-state bias introduced by u_N. Referring to Fig. 3, the 2DOF CNF controller gives considerably better tracking performance compared with the PD-controller. We have also included the performance of a strictly linear measurement feedback controller consisting of the state feedback gain (26), reference tracking gain (27), set point filter (28), and the reduced-order observer with the gain $L_R = 150$.

We see that the lightly damped linear controller does not give satisfactory tracking performance, and the settling time is far worse compared with the 2DOF CNF. We would like to note that the 2DOF CNF controller yields an identical initial transient performance as the strictly linear measurement feedback controller does. However, when the control error $e \to 0$, the nonlinear feedback part of the 2DOF CNF activates. Because of such activation, more control energy is used at the late stage of the transient response, which better utilizes actuator capabilities. As a result, a notch is observed in controller's output, which suppresses overshoot of the linear part. Such feature is the key property of all CNF controllers, which effectively reduce settling time of closed-loop control systems.

Next, we investigate stability properties of the control systems using open-loop frequency responses. For such purpose, we set the reference input $r = 0$, and draw the Nyquist plots of the open-loop systems into Fig. 4. As regards to CNF control, we have included two Nyquist plots, which correspond to 1) the initial system when $\rho = 0$, and 2) the final steady-state system when $\rho = -\beta$. The initial system is identical to the strictly linear measurement feedback system, which smoothly and automatically changes towards the final system when $e \to 0$.
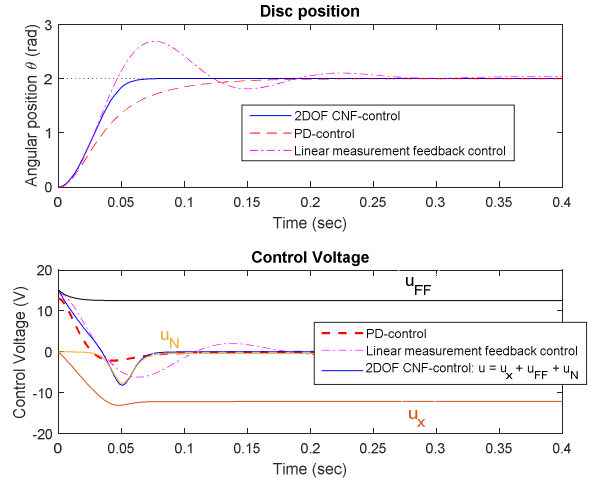

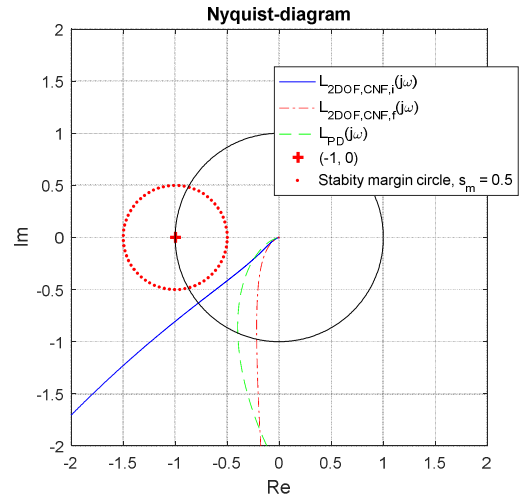Figure 3. Simulation result: tracking performances of closed-loop systems.

Figure 4. Simulation result: open-loop Nyquist-diagram.

According to Fig. 4, all control systems satisfy all frequency domain design constraints. Also, the maximum sensitivities of all control systems are less than 2, because the maximum sensitivity is given by the reciprocal of the stability margin [21]. We would like to note that the set point filter (28) increases the closed-loop bandwidth (BW) from the target reference r to the controlled output y. However, it does not affect to stability properties of the control loop, and hence, the open-loop Nyquist plots are the same regardless of the filter. We can therefore tune the 2DOF CNF controller such that the Nyquist curves stay outside the stability margin circle, and, at the same time, we can speed up the initial stage of the transient response without compromising the control loop robustness.

Nonetheless, we simulate the effect of parameter uncertainties to the closed-loop tracking performances by perturbing the disc load characteristics. To be more specific, we assign ±30% perturbations on the disc mass and disc radius, which change the disc inertia more than ±50%. The step responses of closed-loop control systems under such load perturbations are depicted in Fig. 5. Judging from Fig. 5, the system using 2DOF CNF controller is much better with smaller loads, but the system using PD-controller seems to be better when the load increases.

D. Experimental Results

In this subsection, we test controller performances using the actual device. We reselect $\beta = 0.23$, since we observed small overshoot on the step experiment. Otherwise, we keep the tuning of the 2DOF CNF controller unchanged. The experimentally obtained step responses are collected in Fig. 6. We observe very similar responses as in the previous subsection. However, we want to push the performance of the preceded-derivative PD-controller as good as we can. Performing several tests using the actual equipment, we find that the tuning of the PD-controller can somewhat be improved. The best PD-controller that results in strictly monotone response under the limited control authority is achieved by $K_p = 7.5$, $K_d = 0.23$, and $\omega_f = 150$. The tracking performance of the retuned PD-controller is compared with the 2DOF CNF controller in Fig. 7.
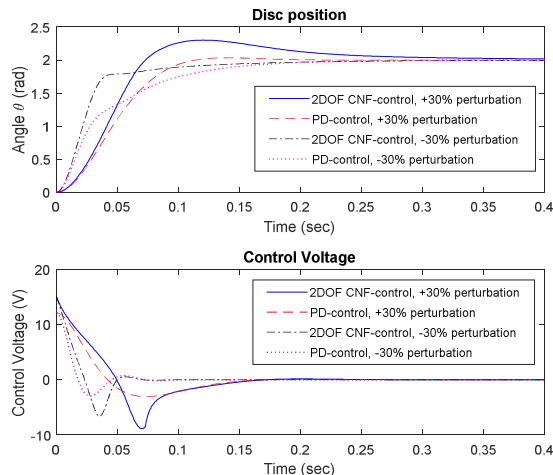

Figure 5.   Simulation result: tracking performances of closed-loop systems under load perturbations.
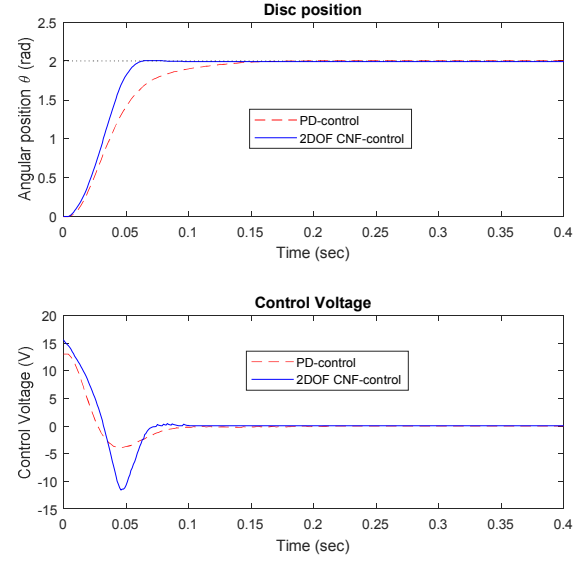

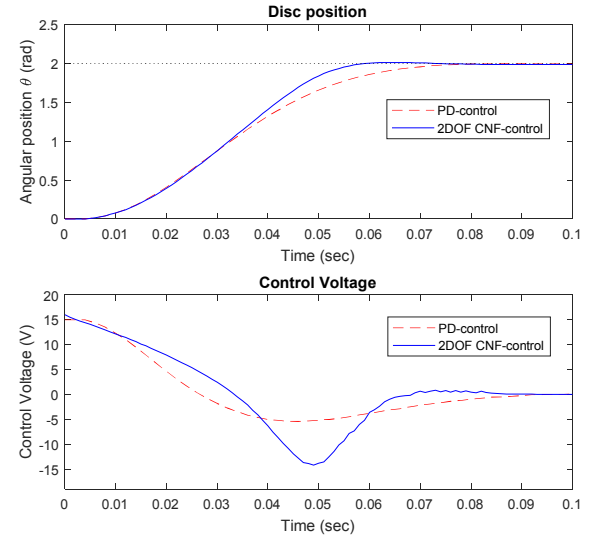Figure 6.   Experimental result: tracking performances of closed-loop systems.

Figure 7.   Experimental result: tracking performances of closed-loop systems with retuned PD-controller.

Referring to Fig. 7, the performance of the PD-controller is clearly improved; although, the settling time is still about 20% slower compared with the 2DOF CNF controller. Attempts to make PD-controller any faster will result in an overshoot, or to saturated actuator. That is, we cannot select the fixed tuning parameter values of the PD-controller such that short settling time and small overshoot could simultaneously be achieved. We also note that the system with retuned PD-controller is more sensitive to load changes, i.e. the set point response is deteriorated with heavier loads.

We have collected all relevant performance measures into Table 2. As regards to 2DOF CNF control, we have included an interval of values for some performance measures. The initial value of the interval corresponds to the initial system when $\rho = 0$. The end value of the interval

TABLE II. QUBE-SERVO 2 PERFORMANCE MEASURES

	2DOF CNF	PD	retuned PD
T_s (ms)	56.8	129.7	71.1
GM	∞	∞	∞
PM (deg)	39.0–77.5	66.5	78.3
s_m	0.63–0.87	0.77	0.83
BW (rad/s)	63.1–125.3	25.7	44.4

corresponds to final system when $\rho = -\beta$. In literature e.g., in [9], the final system characteristics are used to report stability properties of CNF control. We believe that the final system characteristics are more representative than the initial system characteristics are, because the control system is expected to operate most of the time like the final system. The closed-loop system with CNF controller functions as an initial system only instantly when the reference input is changed, and then, the initial system smoothly changes towards the final system.

The bandwidth of the closed-loop system with 2DOF CNF controller also changes significantly between the initial and final systems. Such feature is not surprising, since one pole of the closed-loop system is drawn towards a strictly real stable invariant zero, which is placed relatively close to the imaginary axis. The location of the zero is here determined by the ratio of the gain elements of the nonlinear part. That is, the zero is placed at $s = -1.2375/4.0288 = -0.3072$.

We would like to note that all feedback controllers in this paper have the same dynamic order. However, the 2DOF CNF controller results in better tracking performance, because it has more structural freedom to generate feedback control compared with strictly linear controllers of the same order. Hence, we can conveniently adjust the shape of the responses using additional design freedom under the given constraints and limitations.

IV. CONCLUSION

We have designed in this paper a reduced-order 2DOF CNF controller for a rotary servo system; namely, to a Quanser QUBE-Servo 2 unit with a disc attachment. We compared the performance of our reduced-order 2DOF CNF controller with a carefully tuned preceded-derivative PD-controller. Our simulation and experimental results show that the closed-loop system with the 2DOF CNF controller yields much better set point tracking performance as opposed to the closed-loop system with the PD-controller.

ACKNOWLEDGMENT

REFERENCES

[1] Z. Lin, M. Pachter, and S. Banda, "Toward improvement of tracking performance – nonlinear feedback for linear systems," *Int. J. Contr.*, vol. 70, pp. 1–11, Nov. 1998.

[2] B.M. Chen, T.H. Lee, K. Peng, and V. Venkataramanan, "Composite nonlinear feedback control for linear systems with input saturation: theory and an application," *IEEE Trans. Autom. Contr.*, vol. 48, pp. 427–439, Mar. 2003.

[3] Y. He, B.M. Chen, and C. Wu, "Composite nonlinear control with state and measurement feedback for general multivariable systems with input saturation," *Syst. Contr. Lett.*, vol. 54, pp. 455–469, May 2005.

[4] G. Cheng, K. Peng, B.M. Chen, and T.H. Lee, "Improving transient performance in tracking general references using composite nonlinear feedback control and its application to high-speed XY-table positioning mechanism," *IEEE Trans. Ind. Electron.*, vol. 54, pp. 1039–1051, Apr. 2007.

[5] W. Lan, and B.M. Chen, "On selection of nonlinear gain in composite nonlinear feedback control for a class of linear systems," in *Proc. 46th IEEE Conference on Decision and Control*, New Orleans, LA, USA, Dec. 2007, pp. 1198–1203.

[6] V.-P. Pyrhonen and H. J. Koivisto, "On improvement of transient stage of composite nonlinear feedback control using arbitrary order set point filters," in *Proc. 4th IEEE International Conference on Control System, Computing and Engineering*, Penang, Malaysia, Nov. 2014, pp. 147–152.

[7] B.M. Chen, T.H. Lee, K. Peng, and V. Venkataramanan, *Hard disk drive servo systems*, 2nd ed., Springer, New York, 2006, ch. 5.

[8] V. Venkataramanan, K. Peng, B.M. Chen, and T.H. Lee, "Discrete-time composite nonlinear feedback control with an application in design of a hard disk drive servo system," *IEEE Trans. Contr. Syst. Technol.*, vol. 11, pp. 16–23, Jan. 2003.

[9] K. Peng, B.M. Chen, G. Cheng, and T.H. Lee, "Modeling and compensation of nonlinearities and friction in a micro hard disk drive servo system with nonlinear feedback," *IEEE Trans. Contr. Syst. Technol.*, vol. 13, pp. 708–721, Sep. 2005.

[10] W. Lan, C.K. Thum, and B.M. Chen, "A hard disk drive servo system design using composite nonlinear feedback control with optimal nonlinear gain tuning methods," *IEEE Trans. on Ind. Electron.*, vol. 57, pp. 1735–1745, Sep. 2010.

[11] X. Yu and W. Lan, "Optimal composite nonlinear feedback control for a gantry crane system," in *Proc. 31st Chinese Control Conference*, Hefei, China, July 2012, pp. 601–606.

[12] G. Cai, B.M. Chen, K. Peng, and M. Dong, "Modeling and control of the yaw channel of a UAV helicopter," *IEEE Trans. Ind. Electron.*, vol. 5, pp. 3426–3434, Sep. 2008.

[13] K. Li, K. Wang, K. Zhang, and B.M. Chen, "Aggressive maneuvers of a quadrotor MAV based on composite nonlinear feedback control," in *Proc. 2016 IEEE International Conference on Advanced Intelligent Mechatronics (AIM)*, Banff, Alberta, Canada, July 2016, pp. 513–518.

[14] G. Cai, B.M.Chen, K. Peng, M. Dong, and T.H. Lee, "Design and implementation of a nonlinear flight control law for the yaw channel of a UAV helicopter," in *Proc. 46th IEEE Conference on Decision and Control*, New Orleans, LA, USA, Dec. 2007, pp. 1963–1968.

[15] G. Cheng, and K. Peng, "Robust composite nonlinear feedback control with application to a servo positioning system," *IEEE Trans. Ind. Electron.*, vol. 54, pp.1132–1140, Apr. 2007.

[16] G. Cheng, and J–G. Hu, " An observer-based mode switching control scheme for improved position regulation in servomotors," *IEEE Trans. Contr. Syst. Technol.*, vol. 22, pp. 1883–1891, Dec. 2013.

[17] P. Wendong, and S. Jianbo, "Tracking controller for robot manipulators via composite nonlinear feedback law," *IEEE J. Syst. Eng. Electron.*, vol. 20, pp. 129–135, Jan 2012.

[18] V.-P. Pyrhonen, and H. J. Koivisto, "Gain-scheduled composite nonlinear feedback control of an exothermic chemical reactor," in *Proc. 15th European Control Conference*, Aalborg, Denmark, June–July 2016, pp. 67–73.

[19] J. Apkarian, M. Levis, and P. Martin, "*QUBE-Servo 2 Experiment for MATLAB/Simulink Users – Instructor Workbook*," Quanser Inc. 2016, Ch. PD Control, pp. 5–6.

[20] M. Araki, and H. Taguchi, "Two-degree-of-freedom PID Controllers," *Int. J. Contr., Autom., and Syst.*, vol. 1, pp. 401–411, Dec. 2003.

[21] K.J. Astrom, and T. Hagglund, *Advanced PID Control*, ISA – Instrumentation, Systems, and Automation Society, Research Triangle Park, North Carolina, 2006, pp. 105–113.